Fundamental Gridding Related Dispersion Effects in Multiresolution Time Domain Schemes

Costas D. Sarris and Linda P. B. Katehi

Radiation Laboratory, Department of Electrical Engineering and Computer Science
University of Michigan, Ann Arbor, 48109-2122, MI

Abstract- **The effect of electric and magnetic node arrangement on the dispersion characteristics of the Multiresolution Time Domain technique is investigated in this paper. It is first noted that by multiresolution analysis principles, introducing one wavelet level refines the resolution of a numerical scheme based on scaling functions only, by a factor of two. However, the dispersion analysis of recently formulated MRTD schemes shows that this is not always the case. The apparent contradiction is resolved by indicating that MRTD does achieve its predicted dispersion performance under certain meshing conditions that are outlined here.**

Keywords- **Multiresolution Analysis, numerical dispersion, MRTD, FDTD.**

I. Introduction

The Finite Difference Time Domain (FDTD) technique offers a mathematically straightforward and inherently versatile method for the analysis of arbitrary electromagnetic geometries, at the expense of computational resources. Indeed, since Yee's scheme [1] is second order accurate only, and sensitive to numerical dispersion, a dense discretization of at least ten, but usually twenty five points per wavelength is necessary for the extraction of a convergent solution. Therefore, the FDTD treatment of either electrically large geometries or fine detail structures typically results in a computationally intensive, memory and execution time consuming calculation.

As an alternative to the conventional FDTD, several high order numerical techniques have been developed [2], aiming at the discretization of electromagnetic structures at rates that may even approach the Nyquist limit. Recently, wavelet based time domain methods employing Battle - Lemarie, Daubechies, biorthogonal and Haar wavelets have been presented, for example in [3]-[6] and references therein. It is noted that the introduction of one wavelet level in a numerical scheme formulated with scaling functions only, is expected to bring about a refinement in its effective resolution by a factor of two ("dyadic" property), as a direct consequence of Multiresolution Analysis principles [7]. Nevertheless, in several MRTD dispersion studies [3], [8], the addition of wavelets gives rise to dispersion phenomena that are not consistent with this expectation.

In this paper, the source of the aforementioned contradiction is investigated and the conditions under which MRTD schemes attain their expected dispersion properties are sought for. Such a study is particularly important, for the reason that a future direction of current wavelet research efforts is the development of microwave CAD oriented algorithms. This motivates the assembly of theoretical tools that enable a reliable prediction of the accuracy properties of an MRTD type of scheme, for a given number of wavelet levels and an arbitrary basis.

II. Electric and Magnetic Node Arrangement and Equivalent Grid Points in MRTD

In order to facilitate the presentation of the concepts introduced in this work, the application of the MRTD technique to the simple case of a one dimensional system of Maxwell's equations :

$$\frac{\partial}{\partial t}E_z\left(x,\,t\right) = \frac{1}{\epsilon}\,\frac{\partial}{\partial x}H_y\left(x,\,t\right) \quad (1)$$

$$\frac{\partial}{\partial t}H_y\left(x,\,t\right) = \frac{1}{\mu}\,\frac{\partial}{\partial x}E_z\left(x,\,t\right) \quad (2)$$

is considered. The field update equations are derived by the Method of Moments, in the sense of [3], after a spatial expansion of electric and magnetic field components in scaling and wavelet functions (up to an order r_{max}) is assumed. In the following expressions, $\phi_m(x) = \phi(x/\Delta x - m)$ denotes the scaling function that defines the m-th MRTD cell, the cell size being Δx and $\psi^r_{m,p} = 2^{r/2}\,\psi\left(2^r(x/\Delta x - m) - p\right)$ denotes the p-th wavelet of order r within that cell (with $p = 0, \cdots 2^r - 1$). A temporal basis of pulse functions $h_n(t) = h(t/\Delta t - n)$ is also used (as in [3]). Our treatment is not limited with respect to the wavelet basis, the latter being defined by its scaling and mother wavelet functions, $\phi(x)$ and $\psi(x)$ respectively. The electric and magnetic field expansions are of the form :

$$E_z\left(x,t\right) = \sum_{n,m} h_n(t)\left\{{}_nE^{z,\phi}_m\;\phi_m\left(x\right) + \sum_{r,p}\;{}_nE^{z,\psi_{r,p}}_m\;\psi^r_{m,p}(x)\right\}$$

$$H_y\left(x,t\right) = \sum_{n,m} h_{n'}(t)\left\{{}_{n'}H^{z,\phi}_{m'}\;\phi_{m'}\left(x\right) + \sum_{r,p}\;{}_{n'}H^{z,\psi_{r,p}}_{m'}\;\psi^r_{m',p}(x)\right\} \quad (3)$$

where $n' = n + 1/2$, and $m' = m + s$. Thus, while half a time step offset between the update of electric and magnetic field terms is kept (following the FDTD example), the offset of electric and magnetic field cells is left as a parameter s, under investigation. Most MRTD studies, with the notable exception of [9], use $s = 1/2$. Fig. 1 depicts the equivalent grid points that are generated by this convention, henceforth referred to as **formulation I**, in a 0-order Haar MRTD scheme (one wavelet level). Within each cell, the field values at the "equivalent grid points" are deduced by adding and subtracting the scaling and wavelet terms. It is observed that the electric and magnetic equivalent nodes are now collocated. This kind of mesh condensation happens independently of the basis that is employed and is connected to the dyadic nature of the wavelet transforms of most studies. However, were the resolution refined by a factor

0-7803-6540-2/01/$10.00 (C) 2001 IEEE

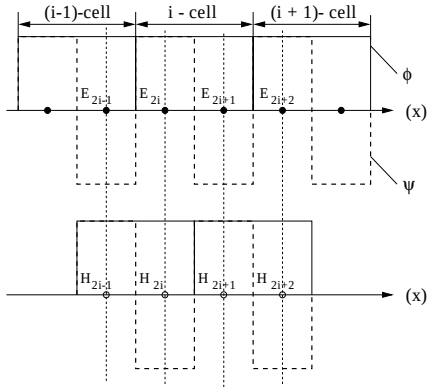

Fig. 1. Electric / magnetic field equivalent grid points for 0 order Haar MRTD, under formulation I.

of two, the offset between these nodes ought to be also divided by two, instead of becoming zero. For a general order scheme, this can be attained by defining $s = 1/2^{r_{max}+2}$, that is, linking s to the maximum wavelet resolution r_{max}. Since the use of wavelets up to order r_{max} renders the effective cell size equal to $\Delta x/2^{r_{max}+1}$, this shift corresponds to half an *effective* cell [10] offset. This convention will be hereafter mentioned as **formulation II**.

III. Dispersion Analysis

A. Battle - Lemarie basis

Following formulation II, the well known W-MRTD scheme of [3] (including Battle-Lemarie scaling and zero order wavelet functions) is rederived (for equations (1)-(2)) and the dispersion properties of its two versions are detemined and compared. Hence, while in [3], the magnetic field basis was composed of functions of the type $\phi_{m+\frac{1}{2}}$, $\psi_{m+\frac{1}{2}}$, the formulation considered here uses accordingly the basis $\phi_{m+\frac{1}{4}}$, $\psi_{m+\frac{1}{4}}$ ($r_{max} = 0$). The discretization of (1), (2) via Galerkin's method leads to finite difference equations of the generic form :

$$\begin{aligned} {}_{n+1}E_m^{z,\phi/\psi} &= {}_{n}E_m^{z,\phi/\psi} \\ &+ \frac{\Delta t}{\epsilon \Delta x} \sum_{p=-p_0}^{p_0-1} \alpha_E^{\phi/\psi}(p)\, {}_{n+\frac{1}{2}}H_{m+p+s}^{y,\phi} \\ &+ \frac{\Delta t}{\epsilon \Delta x} \sum_{p=-p_0}^{p_0-1} \beta_E^{\phi/\psi}(p)\, {}_{n+\frac{1}{2}}H_{m+p+s}^{y,\psi} \end{aligned} \quad (4)$$

and of similar form for the magnetic field. The indicated summations are performed over the "stencil" of the method, denoted here by p_0. The stencil coefficients for the electric and magnetic field $\alpha_E^{\phi/\psi}$, $\beta_E^{\phi/\psi}$, $\alpha_H^{\phi/\psi}$, $\beta_H^{\phi/\psi}$ are not symmetric and some sample values of them are given in Table I. It is noted that $\alpha_E^{\psi}(p) = \beta_E^{\phi}(p-1)$, $\alpha_H^{\psi}(p) = \beta_H^{\phi}(p-1)$.

Subsequently, a dispersion analysis is carried out for W-MRTD under both formulations, by applying the method that is presented in [11]. The resultant dispersion relationships connecting the numerical wavenumber k to the numerical frequency ω are plotted in Fig. 2, where the normalized quantities $X = k\Delta x$ and $\Omega = \omega \Delta t$ have been used. For comparison purposes, the dispersion curves for the so-called S-MRTD (utilizing Battle - Lemarie scaling functions only) and FDTD are also shown. The analytical dispersion curve is indicated as linear. All curves were derived for stencil $p_0 = 9$ and Courant number $\nu = (1/\sqrt{\epsilon\mu})\Delta t/\Delta x$ = 0.15925. Defining the turning point of the dispersion curve as the effective Nyquist limit of the corresponding scheme, it is observed that for S-MRTD this limit is $X = \pi$, for W-MRTD under formulation I it is $X \approx 1.5\pi$, while for W-MRTD under formulation II it is $X = 2\pi$, which shows that the latter does attain the expected refinement in resolution by a factor of two. This is also reflected on the stability condition for the two schemes : For S-MRTD, this condition is $\nu <= 0.6371 = \nu_{S-MRTD}$, for W-MRTD, formulation I $\nu <= 0.4384 = \nu_{W-MRTD-I}$ and for W-MRTD, formulation II $\nu <= 0.3185 = \nu_{W-MRTD-II}$. Hence :

$$\frac{\nu_{S-MRTD}}{\nu_{W-MRTD-I}} \approx 1.4534 \qquad \frac{\nu_{S-MRTD}}{\nu_{W-MRTD-II}} \approx 2.0 \quad (5)$$

Thus, the previous conclusion is verified from a stability perspective : The addition of wavelets under the node arrangement of formulation I brings about a mesh refinement of less than 1.5, while formulation II leads to a full exploitation of the wavelets, doubling the resolution of S-MRTD.

TABLE I
Stencil Coefficients for the W-MRTD Scheme (formulation II)

p	$\alpha_E^{\phi}(p)$	$\beta_E^{\phi}(p)$	$\alpha_E^{\psi}(p)$
-5	-5.596e-02	-7.607e-02	+5.864e-02
-4	+0.1051694	+0.1403895	-9.579e-02
-3	-0.2015483	-0.2474964	+0.2343052
-2	+0.4196303	+0.3727935	-0.3023901
-1	-1.3241406	-0.4279963	+1.9484456
0	+0.7974678	+0.3594450	+4.3699193
+1	+0.3590904	-0.2313141	-0.1205340
+2	-0.1816382	+0.1289039	+0.2431251
+3	+9.570e-02	-6.952e-02	-7.818e-02
+4	-5.103e-02	+3.727e-02	+5.605e-02
+5	+2.729e-02	-1.996e-02	-2.585e-02

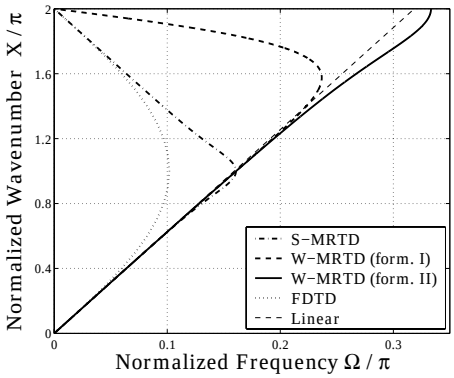

Fig. 2. Dispersion curves for W-MRTD (formulations I, II), S-MRTD and FDTD.

B. Haar basis

The relative simplicity of the Haar basis allows for the derivation and dispersion analysis of an arbitrary order scheme applied to equations (1), (2). The update equations of the scheme are derived by applying the Method of Moments, considering field expansions according to formulations I, II. As an example, the

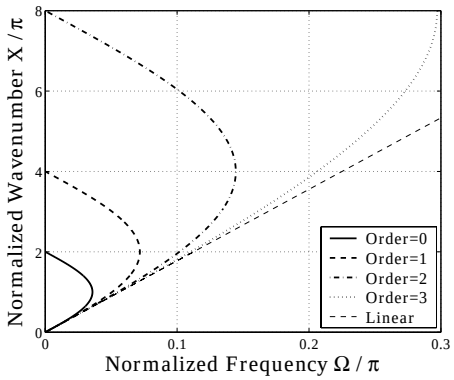

Fig. 3. Dispersion curves for Haar MRTD of orders 0 to 3, under formulation I.

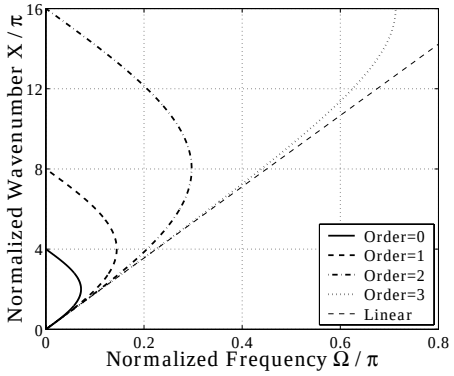

Fig. 4. Dispersion curves for Haar MRTD of orders 0 to 3, under formulation II.

update equation for the electric field scaling terms assumes the form :

$$ {}_{n+1}E_m^{z,\phi} = {}_nE_m^{z,\phi} + \frac{\Delta t}{\epsilon\,\Delta x}\left\{ {}_{n+\frac{1}{2}}H_{m+s}^{y,\phi} - {}_{n+\frac{1}{2}}H_{m+s-1}^{y,\phi} + \sum_{r=0}^{r_{max}} 2^{r/2}\left({}_{n+\frac{1}{2}}H_{m+s}^{y,\psi_{r,2^r-1}} - {}_{n+\frac{1}{2}}H_{m+s-1}^{y,\psi_{r,2^r-1}}\right)\right\} \quad (6) $$

The dispersion analysis of the two formulations leads to the following closed form expressions : For formulation I,

$$ \frac{1}{\nu^2}\,\sin^2\frac{\Omega}{2} = 2^{2\,r_{max}}\sin^2\left(X/2^{r_{max}+1}\right) \quad (7) $$

and for formulation II :

$$ \frac{1}{\nu^2}\,\sin^2\frac{\Omega}{2} = 2^{2\,r_{max}+2}\sin^2\left(X/2^{r_{max}+2}\right) \quad (8) $$

The resultant curves are depicted in Figures 3, 4 for $\nu = 0.05625$. It is thus shown that MRTD under formulation I, always finds itself one level of resolution below the expected, while MRTD under formulation II exhibits a consistent dispersion performance. For example, for $r_{max} = 0$, (7) yields the FDTD dispersion equation, corresponding to the scaling cell resolution (the addition of wavelets does not change the accuracy of the scheme). In this case, actually, the MRTD scaling and wavelet update equations are uncoupled and whatever improvement in accuracy is solely due to the application of source or boundary conditions [8].

IV. Numerical Results

A. Battle - Lemarie basis

A simple numerical experiment that validates the dispersion analysis of the two W-MRTD schemes is carried out in this section. In particular, a computational domain defined by 200 Battle - Lemarie scaling cells terminated into hard boundary conditions (implemented by image theory) is solved as a one dimensional cavity. Then, the resonant frequencies $f_n = 0.15\,n$ [GHz] of the cavity, corresponding to normalized wavenumbers $X_n = 0.01\pi n$ are numerically determined, from time domain data of 32768 time steps. For both schemes, a time step equal to 0.5 of their stability limit is used, for the results to be directly comparable. The stencil value p_0 is set to 12. Results

TABLE II
Resonant Frequencies (in GHz) for the 1-D Cavity Problem and Relative Error for W-MRTD (I,II)

$\frac{X_n}{\pi}$	f_n	W-MRTD Form.I	R.E. (%)	W-MRTD Form.II	R.E. (%)
0.2	3	3.0018	+0.0600	2.9989	-0.0037
0.4	6	6.0351	+0.5850	6.0035	+0.0058
0.6	9	9.1345	+1.4944	9.0139	+0.1544
0.8	12	12.4179	+3.4825	12.0071	+0.0592
1.0	15	15.6897	+4.5980	15.0979	+0.6527
1.2	18	19.2975	+7.2083	18.2749	+1.5727
1.4	21	22.6670	+7.9381	21.5725	+2.7262
1.6	24	24.3158	+1.3158	25.1689	+4.8704
1.8	27	18.0221	-33.2515	29.1010	+7.7815

for wavenumbers ranging from 0 to 2π are listed in Table II. It is clearly shown that W-MRTD under formulation II is consistently more accurate than formulation I, except for wavenumbers around the effective Nyquist limit of formulation I, where its error changes sign and therefore assumes values close to zero. However, from that point on, the accuracy difference between the two schemes becomes significant. For example, when $X = 1.8\pi$, formulation I yields an alias frequency, presenting a relative error of -33.2515 %. As discussed in [12], this frequency is a product of inaccuracy, not a spurious mode, as was previously misinterpreted [3].

Furthermore, to demonstrate the equivalence of the proposed W-MRTD scheme to the S-MRTD based on Battle Lemarie scaling functions of *double* resolution (that span the so called space $V_1 = V_0 \oplus W_0$), the previous cavity domain is solved with the latter scheme and the relative error in the deduced frequencies for wavenumbers π to 2π is plotted in Fig. 5. A good agreement between the two schemes under comparison is observed. It is noted that any (numerically small) discrepancies represent the effect of the boundary condition modeling and the truncation of the scheme (by the choice of a finite stencil).

B. Haar basis

Extending the arbitrary order Haar MRTD scheme to two dimensions, the FDTD and MRTD (formulations I, II) solutions for the $TE_{n,m}$ modes of a square air cavity structure of dimensions $32\ cm \times 32\ cm$ are compared. The Haar MRTD schemes of orders 2 by 2, 3 by 3 and 4 by 4, corresponding to meshes of 4×4, 2×2 and 1×1 scaling cells are applied to the structure,

0-7803-6540-2/01/$10.00 (C) 2001 IEEE

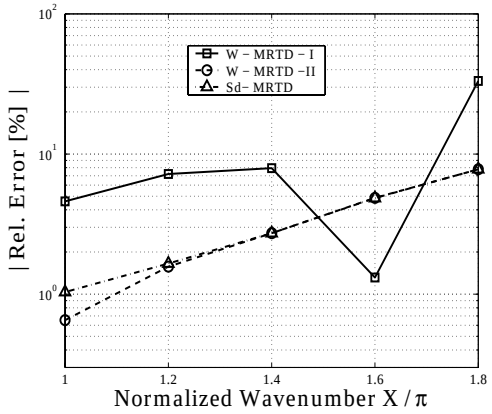

Fig. 5. Relative errors in resonant frequency for W-MRTD I, II and S-MRTD of the "next" level of resolution (denoted as "S_d").

TABLE III
RESONANT FREQUENCIES (IN GHZ) FOR THE 2-D CAVITY PROBLEM AND RELATIVE ERROR (DEGREES OF FREEDOM = 32×32)

(n,m)	$f_{n,m}$	MRTD form.I	R.E. (%)	MRTD form.II	R.E. (%)
(1,1)	0.6629	0.6620	-0.1358	0.6627	-0.0030
(2,1)	1.0482	1.0451	-0.2957	1.0466	-0.1526
(2,2)	1.3258	1.3233	-0.1886	1.3240	-0.1357
(3,1)	1.4823	1.4714	-0.7353	1.4793	-0.2024
(3,2)	1.6901	1.6827	-0.4378	1.6878	-0.1361
(3,3)	1.9887	1.9818	-0.3470	1.9853	-0.1709

along with a 32×32 cell FDTD. The hard boundary conditions are modeled in MRTD by applying image theory for the update of magnetic field coefficients at the boundaries, in the sense developed in [13]. Under these gridding conditions, our dispersion analysis yields that FDTD and MRTD (formulation II) have the same accuracy, as they use the same number of degrees of freedom (thresholding is not applied in this study). This has been also numerically confirmed ; the resonant frequencies deduced by FDTD and all MRTD schemes of formulation II, assume the $same$ arithmetic values, some of which are given in Table III. However, formulation I shows a significantly worse accuracy, following that of an FDTD scheme of a 16×16 mesh. All simulations were carried out at 0.9 of the stability limit for each scheme. It is thus concluded that Haar MRTD under formulation II attains its expected resolution, just as the dispersion analysis showed and in contradiction to formulation I. Finally, Fig. 6 depicts the electric field spatial distribution of the TE_{32} mode of the cavity as resolved by a 1×1 mesh of an order 4 by order 4 (5 wavelet levels per direction) Haar MRTD scheme (formulation II).

V. CONCLUSIONS

A necessary condition for the development of MRTD schemes with a consistent accuracy performance has been derived by means of dispersion analysis and confirmed by numerical experiments. It is also noted that under the same condition, the two different methods of deriving wavelet schemes presented in the microwave literature so far [3], [4] become equivalent. Thus, this work contributes to the fundamental understanding of the numerical properties of wavelet schemes and their connection to Multiresolution Analysis principles.

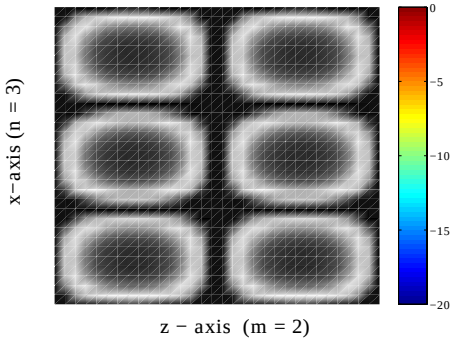

Fig. 6. Electric field distribution for TE_{32} mode obtained by an order 4 by order 4 Haar MRTD (form. II), with a 1 by 1 mesh.

VI. ACKNOWLEDGMENTS

The research reported in this paper was initially inspired by a preprint of [9] that Prof. L. Carin of Duke University provided to the authors. This important contribution is gratefully acknowledged.

This research has been supported by the Army Research Office under the project for "Efficient Numerical Solutions to Large Scale Tactical Communication Problems" (DAAD19-00-1-0173).

REFERENCES

[1] K. S. Yee, "Numerical solution of initial boundary value problems involving Maxwell's equations in isotropic media", *IEEE Trans. Antennas Prop., vol. 14, no. 3, pp. 302-307, March 1966.*

[2] A. Taflove, *Advances in Computational Electrodynamics : The Finite Difference Time Domain Method* , Artech House, 1998.

[3] M. Krumpholz, L.P.B. Katehi, "MRTD: New Time Domain Schemes Based on Multiresolution Analysis", *IEEE Trans. Microwave Theory and Techniques, vol.44, no.4, pp.555-561, April 1996.*

[4] W. Werthen and I. Wolff, "A novel wavelet based time domain simulation approach", *IEEE Microwave and Guided Wave Lett., vol. 6, no. 12, pp. 438-440, Dec. 1996.*

[5] M. Aidam and P. Russer, "Application of biorthogonal B - spline wavelets to Telegrapher's equations", *Proc. of the 14th Annual Review of Progress in Applied Computational Electromagnetics, pp. 983-990, Monterey, CA, March 1998.*

[6] M. Fujii and W. J. R. Hoefer, "A three-dimensional Haar wavelet-based multi-resolution analysis similar to the 3-D FDTD method - derivation and application", *IEEE Trans. Microwave Theory Tech., vol. 46, no. 12, pp. 2463-2475, Dec. 1998.*

[7] I. Daubechies, *Ten Lectures on Wavelets*, SIAM Rev., Philadelphia, PA, 1992.

[8] M. Fujii and W. J. R. Hoefer, "Numerical Dispersion in Haar wavelet based MRTD scheme - Comparison between analytical and numerical results", *Proc. 15th Annual Review of Progress in Applied Computational Electromagnetics, pp. 602-607, Monterey, CA, March 1999.*

[9] T. Dogaru and L. Carin, "Application of Multiresolution Time Domain Schemes to two dimensional Electromagnetic Scattering Problems", *submitted to IEEE Trans. Antennas Prop., 1999.*

[10] C. D. Sarris, L. P. B. Katehi, "On the use of wavelets for the implementation of high order mesh refinement in time domain simulations", *Proceedings of the 30th European Microwwave Conference, pp. 284-287, Paris, France, October 2000.*

[11] C. D. Sarris, L. P. B. Katehi, "Some Aspects of Dispersion Analysis of MRTD Schemes", *2001 Review of Progress in Applied Computational Electromagnetics, submitted.*

[12] C. D. Sarris, L. P. B. Katehi, "On the Existence of Spurious Modes in Battle-Lemarie Based MRTD", *IEEE Microwave and Guided Wave Letters, submitted, October 2000.*

[13] C. D. Sarris and L. P. B. Katehi, "Formulation and Study of an Arbitrary Order Haar Wavelet Based MRTD technique *Proceedings of the 216th Annual Review of Progress in Applied Computational Electromagnetics, pp.540-547, Monterey, CA, March 2000.*